THE JOURNAL OF BIOLOGICAL CHEMISTRY VOL. 287, NO. 39, pp. 32354–32366, September 21, 2012

The Acid-sensitive, Anesthetic-activated Potassium Leak Channel, KCNK3, Is Regulated by 14-3-3β-dependent, Protein Kinase C (PKC)-mediated Endocytic Trafficking*

Received for publication, June 14, 2012, and in revised form, July 27, 2012 Published, JBC Papers in Press, July 30, 2012, DOI 10.1074/jbc.M112.391458

Luke Gabriel[‡§], **Anatoli Lvov**[¶], **Demetra Orthodoxou**[§], **Ann R. Rittenhouse**[‡‖], **William R. Kobertz**[‡¶], **and Haley E. Melikian**[‡§1]

From the [‡]*Graduate Program in Neuroscience,* [¶]*Department of Biochemistry and Molecular Pharmacology,* [‖]*Department of Microbiology and Physiological Systems, and* [§]*Brudnick Neuropsychiatric Research Institute, Department of Psychiatry, University of Massachusetts Medical School, Worcester, Massachusetts 01604*

Background: KCNK3 is an anesthetic-activated K^+ leak channel that sets the neuronal resting membrane potential.
Results: PKC activation rapidly decreases KCNK3 surface levels, and KNCK3 surface losses require a non-classical endocytic signal and 14-3-3β.
Conclusion: KNCK3 activity is acutely regulated by endocytic trafficking.
Significance: This is the first demonstration that endocytosis regulates KCNK3 activity and that 14-3-3β is required for neuronal endocytic trafficking.

The acid-sensitive neuronal potassium leak channel, KCNK3, is vital for setting the resting membrane potential and is the primary target for volatile anesthetics. Recent reports demonstrate that KCNK3 activity is down-regulated by PKC; however, the mechanisms responsible for PKC-induced KCNK3 down-regulation are undefined. Here, we report that endocytic trafficking dynamically regulates KCNK3 activity. Phorbol esters and Group I metabotropic glutamate receptor (mGluR) activation acutely decreased both native and recombinant KCNK3 currents with concomitant KCNK3 surface losses in cerebellar granule neurons and cell lines. PKC-mediated KCNK3 internalization required the presence of both 14-3-3β and a novel potassium channel endocytic motif, because depleting either 14-3-3β protein levels or ablating the endocytic motif completely abrogated PKC-regulated KCNK3 trafficking. These results demonstrate that neuronal potassium leak channels are not static membrane residents but are subject to 14-3-3β-dependent regulated trafficking, providing a straightforward mechanism to modulate neuronal excitability and synaptic plasticity by Group I mGluRs.

Potassium (K^+) leak channels are major determinants of neuronal membrane potential and excitability (1, 2). "2P" K^+ channels are composed of two monomers, each with two pore-forming domains (3–7), as opposed to tetrameric K^+ channels, with each monomer contributing two pores (8, 9). KCNK3 (TASK-1) channels are widely expressed, with enriched expression reported in motor neurons (10), cerebellar granule neurons (10, 11), and the carotid body (12). KCNK3 assembles as a functional homo- or heterodimer with its homolog KCNK9 (13–15). Both KCNK3 homo- and heterodimers are acid-sensitive (14, 16) and are activated by volatile anesthetics (17, 18), which decrease spontaneous neuronal firing rates (17–21). KCNK3 is also inhibited by sanshool (22), the Szechuan peppercorn component that induces a numbing sensation. Studies with KCNK3(−/−) mice demonstrated that KCNK3 is critical for neuroprotection during stroke (23); for chemosensory control of breathing (24); and for adrenal cortex development, aldosterone production, and response to increased dietary sodium intake (25). Taken together, KCNK3 plays a major role in a number of physiological functions throughout the CNS and periphery, and mechanisms that alter KCNK3 function and availability are likely to have a significant systemic impact.

Multiple regulatory proteins control KCNK3 maturation and surface expression. *In vitro* studies demonstrate C-terminal KNCK3 phosphorylation by PKA correlated to enhanced KCNK3 surface expression, presumably by increased forward trafficking from the ER[2] (26). In contrast, βCOP binds to the KCNK3 N terminus and prevents egress from the ER and Golgi to the plasma membrane (27). The KCNK3/βCOP protein-protein interaction can be mitigated by p11 and 14-3-3β, both of which bind to the KCNK3 C terminus and increase KCNK3 forward trafficking (27–30).

Mounting evidence demonstrates that KCNK3 activity is acutely regulated, via either protein kinase C (PKC) (31) or G_q-coupled receptor activation (19, 32–34). However, the mechanisms mediating KCNK3 regulation are completely unknown. In the current study, we show that PKC-regulated endocytic trafficking acutely modulates KCNK3. KCNK3 C-terminal res-

* This work was supported, in whole or in part, by National Institutes of Health Grants DA15169 (to H. E. M.) and GM070650 (to W. R. K.). This work was also supported by the University of Massachusetts Center for AIDS Research (to H. E. M. and W. R. K.).

[1] To whom correspondence should be addressed: Brudnick Neuropsychiatric Research Institute, Dept. of Psychiatry, University of Massachusetts Medical School, 303 Belmont St., Worcester, MA 01604. Tel.: 508-856-4045; Fax: 508-856-2627; E-mail: haley.melikian@umassmed.edu.

[2] The abbreviations used are: ER, endoplasmic reticulum; PMA, phorbol 12-myristate 13-acetate; REK/AAA, R335A/E336A/K337A; TEA, triethylammonium; TTX, tetrodotoxin; DHPG, (*S*)-3,5-dihydroxyphenylglycine; Tf, transferrin; TfR, Tf receptor; DAT, dopamine transporter; BIM, bisindolylmaleimide.

idues are critical for KCNK3 endocytosis and define a novel K^+ channel endocytic signal. Moreover, we demonstrate that 14-3-3β is absolutely required for KCNK3 internalization, a role heretofore not described for a 14-3-3 protein. These results demonstrate that KCNK3 is not static in the plasma membrane but is dynamically trafficked, enabling potassium leak channels to acutely modulate neuronal excitability and potentially contribute to synaptic plasticity.

EXPERIMENTAL PROCEDURES

cDNA Constructs

Rat KCNK3 cDNA was the generous gift of Dr. Joseph Cotton (Massachusetts General Hospital, Boston, MA) and was subcloned into pcDNA 3.1(+). HA-KCNK3 was the generous gift of Dr. Douglas Bayliss (University of Virginia), and human 14-3-3β-GFP-C1 cDNA was the gift of Dr. Mitsuo Ikebe (University of Massachusetts Medical School). KCNK3 point mutants were generated using the QuikChange mutagenesis kit (Stratagene), and mutant cDNA regions were subcloned back into the wild type KCNK3 plasmids at XcmI/XbaI sites. All mutations were confirmed by dideoxynucleotide cycle sequencing (GeneWiz, South Plainfield, NJ). shRNA constructs were purchased from Origene (Rockville, MD).

Cell Culture and Transfections

HEK 293T cells were cultured at 37 °C, 5% CO_2 in high glucose DMEM supplemented with 10% fetal bovine serum, 2 mM L-glutamine, and penicillin/streptomycin. For transfections, HEK cells were seeded in 6-well cultureware 1 day prior to transfection, were transiently transfected with Lipofectamine 2000 according to the manufacturer's instructions (Invitrogen), and were assayed 48 h post-transfection. For wide field microscopy, cells were replated onto poly-D-lysine-coated glass coverslips 24 h post-transfection. For knockdown experiments, KCNK3 cDNA and shRNA plasmids were co-transfected into HEK cells and assayed 48 or 72 h post-transfection.

Cerebellar Granule Neuron (CGN) Isolation

P6 Sprague-Dawley rat pups were sacrificed, and their cerebella were surgically removed, minced, and incubated in 0.05% trypsin for 10 min under carbogen at 37 °C. Following trypsinization, tissue was washed three times in CTPM (α-minimum Eagle's medium supplemented with B27, 10 units/ml penicillin/streptomycin, 250 kilounits/ml DNase I, 25 mM KCl, 6 mg/ml glucose) and was dissociated by triturating progressively through 21–26-gauge needle holes in flame-sealed P1000 pipette tips. Cells were collected by centrifugation (1000 × *g*, 5 min), resuspended in CTPM, and plated on 25 μg/ml poly-D-lysine-coated glass coverslips (4 × 104 cells/well) or in 12-well cultureware (7.5 × 105 cells/well) for electrophysiological and biochemical assays, respectively. Cells were grown at 37 °C at 5% CO_2 for 5 h, and the medium was changed to Neurobasal medium (Invitrogen) supplemented with B27, 10 units/ml penicillin/streptomycin, 2 mM glutamine, and 25 mM KCl. Neurons were assayed at 4–13 days *in vitro*.

Electrophysiological Recordings

HEK Cells—Cells were transiently transfected with recombinant cDNA clones of KCNK3 or KCNK9 channel (0.2 μg), green fluorescent protein (pEGFP-C1; 0.25 μg), and empty plasmid (pcDNA3.1(-), 0.55 μg) using 4 μl of Lipofectamine and 6 μl of PLUS™ reagent (Invitrogen). For shRNA experiments, 2 μg of DNA (1 μg of shRNA, 0.2 μg of channel, 0.8 μg of pcDNA3.1) and 4 μl of Lipofectamine were used. After terminating the transfections (4 h), cells were reseeded onto 8-mm round coverglasses (Warner Instruments) and incubated for an additional 24–48 h. K^+ currents were recorded at room temperature (24 ± 2 °C) from voltage-clamped cells. The recording chamber was continuously perfused with extracellular (bath) solution that contained 160 mM NaCl, 2.5 mM KCl, 2 mM $CaCl_2$, 1 mM $MgCl_2$, 8 mM glucose, and 10 mM HEPES (pH 7.5 with NaOH). Patch electrode tip resistance was 1–3 megaohms when filled with intracellular (electrode) solution that contained 126 mM KCl, 20 mM NaCl, 0.5 mM $MgCl_2$, 0.1 mM EGTA, 0.5 mM ATP-Na_2, 0.3 mM GTP-Na_3, 10 mM HEPES (pH 7.5 with KOH). Transfected (pEGFP-expressing) cells were identified using a GFP filter set of the Axiovert 40 CFL inverted light microscope (Zeiss). Currents were assayed for native-like function using a "family" of traces protocol, in which a cell held at −80 mV was stepped for 50 ms every 15 s to potentials between −120 and +45 mV in 15-mV increments, followed by a 20-ms command to −120 mV. The effect of PKC activation on the current was studied using phorbol 12-myristate 13-acetate (PMA, Tocris Bioscience), which was dissolved in ethanol and diluted in bath solution to 1 μM (0.006% final ethanol concentration). Current amplitude *versus* time was monitored by holding cells at −80 mV and recording the current during a 50-ms test depolarization (40 mV) every 30 s.

CGNs—Leak current from 5–14-day *in vitro* CGNs were recorded at room temperature (22–24 °C) using the whole-cell configuration of an Axopatch 200B patch clamp amplifier (Axon Instruments, Foster City, CA). Electrodes were pulled from borosilicate glass capillaries (Drummond Scientific Co., Broomall, PA) and fire-polished to a tip diameter of ~1 μm. The total pipette access resistance ranged from 2.0 to 2.5 megaohms. Cells were held at −20 mV to inactive voltage-activated Ca^{2+}, Na^+, and K^+ channels. Currents were elicited every 10 s by stepping from −20 mV to various test potentials for 50 ms using the CED Signal software suite, version 2.15 (Cambridge Electronic Design, Cambridge, UK). Currents were filtered at 5 kHz using the amplifier's four-pole, low pass Bessel filter, digitized at 20 kHz with a micro1401 interface (CED), and stored on a personal computer. Electrodes were filled with internal solution containing 140 mM KCl, 4 mM NaCl, 10 mM HEPES, 10 mM EGTA, 5 mM $MgCl_2$, 4 mM ATP, 0.4 mM GTP, pH 7.5. Cells were patched in calcium Tyrode's solution containing 145 mM NaCl, 5.4 mM KCl, 5 mM $CaCl_2$, 10 mM HEPES with the pH adjusted to 7.5. After rupturing the cell membrane, the bath solution was exchanged by a gravity-fed perfusion system. The external solution contained 140 mM NaCl, 3 mM KCl, 10 mM HEPES, 10 mM glucose, 2 mM $MgCl_2$, 2 mM $CaCl_2$, 10 mM TEA, 0.0005 mM tetrodotoxin (TTX), pH 7.5. TEA and TTX were included in the bath solution to inhibit K_{Ca} current and

any residual Na_v current, respectively. To activate PKC, PMA (1 μM) or (*S*)-3,5-dihydroxyphenylglycine (DHPG) (1 μM) was added to the bath after 2 min of measuring stable currents.

Data Analysis—Leak current amplitudes were measured at −20 mV and plotted over time in the presence of agonist for at least 15 min. At this potential, many voltage-gated ion channels in neurons are inactivated, and thus the current is highly enriched in leak channel current. Moreover at −20 mV, the current-voltage relationship is in the linear range, where any changes in current amplitude will be most obvious. Only cells that had a control leak current reversal potential more negative than −40 mV were used in the analyses. Significance of the action of PMA or DHPG was determined using a two-tailed paired *t* test.

Cell Surface Biotinylation

Cells were treated as described, and surface proteins were covalently labeled with sulfosuccinimidyl 2-(biotinamido)-ethyl-1,3-dithiopropionate as described previously (35). Cells were lysed in 3.2 mM dodecyl maltoside, 50 mM Tris, pH 7.4, 150 mM NaCl, 2 mM EDTA, 1 μg/ml leupeptin, 1 μg/ml pepstatin, 1 μg/ml aprotinin, and 1 mM PMSF for 20 min at 4 °C, and protein concentrations were determined using the BCA protein assay (Pierce). Biotinylated proteins were isolated by batch streptavidin chromatography (overnight, 4 °C), and bound proteins were eluted in 30 μl of 3× Laemmli SDS-PAGE sample buffer with 10% SDS for 15 min at room temperature. Surface proteins and one-half of the total cellular lysate were resolved on 10% SDS-PAGE and transferred to nitrocellulose, and KCNK3 was detected by immunoblotting using rat anti-HA antibody (clone 3F10, Roche Applied Science). Immunoreactive bands were detected using a VersaDoc CCD camera system, and non-saturating bands were quantified using Quantity One software (Bio-Rad).

Wide Field Microscopy

Cells were transfected in 6-well dishes and, 24 h post-transfection, were trypsinized and replated on poly-D-lysine-coated plates. 48 h post-transfection, cells were treated as indicated, rinsed in PBS, and fixed in 4% paraformaldehyde prepared in PBS for 10 min at 25 °C. For Tac surface labeling, cells were incubated with mouse anti-IL2aR antibodies (Millipore) (1:2000) for 2 h at 4 °C prior to fixation and permeabilization. For transferrin (Tf) co-localization experiments, cells were loaded with 20 ng/μl Tf-Alexa594 during drug treatments. Cells were blocked and permeabilized in blocking solution (PBS, 1% IgG/protease-free BSA, 5% goat serum, 0.2% Triton X-100) for 30 min at room temperature, followed by incubation with the indicated primary antibodies for 45 min at 25 °C. Cells were washed with PBS and incubated with Alexa594- or Alexa488-conjugated secondary antibodies (as indicated; Invitrogen) for 45 min at 25 °C. Cells were washed with PBS, dried, and mounted on glass slides with ProLong Gold mounting medium (Molecular Probes). Immunoreactive cells were visualized as described previously (36) with a Zeiss Axiovert 200 M microscope using a ×63, 1.4 numerical aperture oil immersion objective, and 0.4-μm optical sections were captured through the *z* axis with a Retiga-1300R cooled CCD camera (Qimaging) using Slidebook 5.0 software (Intelligent Imaging Innovations, Denver, CO). *z* stacks were deconvolved with a constrained iterative algorithm using measured point spread functions for each fluorescent channel. All images shown are single 0.4-μm planes through the center of each cell. For quantification, the plasma membrane was defined independent of KCNK3 staining by masking the Tac signal in the Alexa488 channel. KCNK3 surface signal intensities in the Alexa594 channel were then measured within the mask, and total KCNK3 cell signal intensities were measured by filling in the mask within the cell. Data are the average of four cells/condition/experiment, quantified over three independent experiments.

RESULTS

KCNK3 Currents Are Down-regulated by PKC Activation—Previous studies reported PKC-dependent losses in KCNK3 currents in heterologous expression systems (31) and cardiac myocytes (37). Given that the KCNK3 C terminus encodes SREKLQYSIP, a sequence homologous to the dopamine transporter (DAT) PKC-regulated endocytic signal, FREKLAYAIA, we hypothesized that KCNK3 may undergo PKC-mediated endocytic trafficking as a means to acutely regulate KCNK3 function. To test this possibility, we first asked whether PKC-mediated KCNK3 down-regulation occurred in neurons, by measuring whole cell leak current in CGNs, in which KCNK3 is endogenously expressed (10, 11). Upon blocking Na_v^+ currents with TTX and K_{ca} currents with TEA, we detected acid-sensitive (Fig. 1*A*) and Zn^{2+}-sensitive (Fig. 1*B*) components of the leak current, indicating native KCNK3 and KCNK9 expression, respectively, as observed previously in CGNs (15). The individual traces shown in Fig. 1*C* illustrate the decrease in leak current amplitude of CGNs following 15 min of treatment with 1 μM PMA. The average decrease in current amplitude over time can be observed and contrasted with currents recorded in the presence of vehicle, which remained stable over 15 min (Fig. 1*E*). Consequently, after 15 min of PMA, 63 ± 10% (Fig. 1, *C–E*) of the leak current remained, and this decrease in amplitude was significantly different from that in vehicle-treated cells (99 ± 13%) as shown in the summary *bar graph* in Fig. 1*D* ($p < 0.05$; two-way Student's *t* test for two means; $n = 8–9$/group).

Because CGNs express both KCNK3 and KCNK9 subunits, we next determined whether the PKC-mediated inhibition of the acid-sensitive leak current in neurons was specific for one of the KCNK subunits. Native acid-sensitive leak currents are generated by homo- and heterodimers composed of KCNK3 and its homolog, KCNK9 (14, 15). KCNK9 is 82% identical to KCNK3; however, their C termini are highly divergent, and KCNK9 does not encode a SREKLQYSIP endocytic motif. Transient expression of KCNK3 in HEK293T cells resulted in robust, acid-sensitive currents in the whole-cell patch clamp configuration (data not shown). Treatment with 1 μM PMA decreased KCNK3 currents to 64.1 ± 3.4% of base-line levels by 15 min (Fig. 2*A*), which was significantly lower than currents measured in vehicle-treated cells (101.6 ± 5.2% base line; $p < 0.001$; Student's *t* test; $n = 3–5$). In contrast, PMA had no effect on KCNK9 currents (vehicle = 84.8 ± 7.8% base line; PMA = 82.9 ± 3.6% base line; $p = 0.89$; Student's *t* test; $n = 3$) (Fig. 2*B*). These results suggested that the PMA-induced losses in acid-

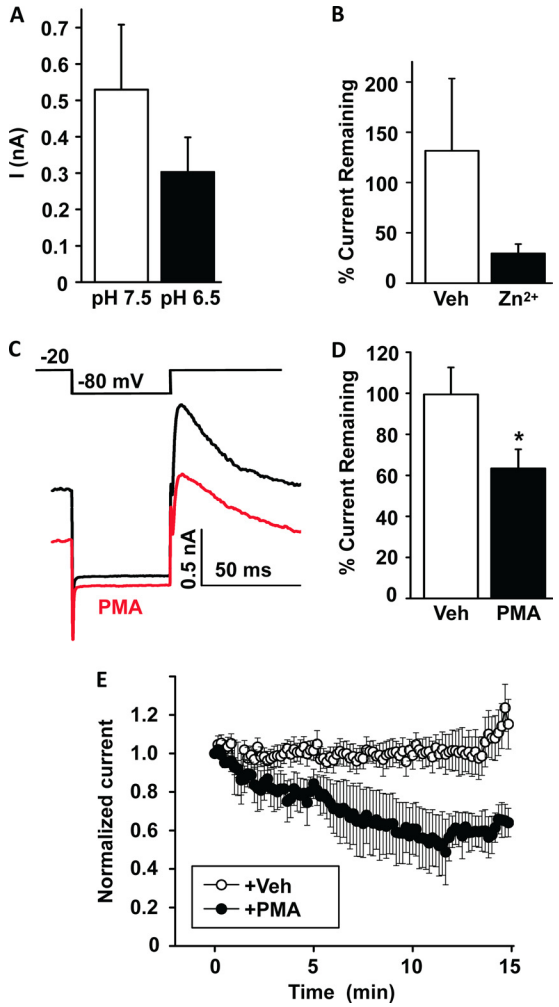

FIGURE 1. **PKC activation decreases acid-sensitive currents in CGNs.** Shown are whole-cell recordings of K^+ leak current in the presence of 0.5 μM TTX and 10 mM TEA. *A*, average decrease in current amplitude following bath solution exchange from pH 7.5 to 6.5 ($n = 7$). *B*, zinc sensitivity following introduction of 100 μM zinc (Zn^{2+}) ($n = 5$). *C*, representative traces of leak current at time 0 min (*black line*) and 15 min following 1 μM PMA (*red line*). *D*, average percentage of current remaining after 15 min with 1 μM PMA is significantly different from that with an equal volume of vehicle (*Veh*) added to the bath solution. *, $p < 0.05$; Student's *t* test; $n = 8$–9/group. *E*, average normalized time courses of leak current following introduction of either vehicle (○) or 1 μM PMA (●) into the bath at time 0. Currents were sampled every 10 s ($n = 8$–9/group). *Error bars*, S.E.

sensitive leak current in CGNs were specific for channels containing the KCNK3 subunit.

KCNK3 Internalizes in Response to PKC Activation—PKC-mediated losses in KCNK3 currents could be due to changes in channel conductance, open probability, or surface number due to acute endocytic trafficking, as opposed to forward trafficking from the ER as described previously (27, 28). However, the time course of KCNK3 down-regulation in response to PKC activation occurred over minutes, consistent with an endocytic trafficking event. Therefore, we used surface biotinylation to ask whether PKC-mediated KCNK3 functional losses were due to KCNK3 protein losses at the cell surface. We first attempted to use a commercially available anti-KCNK3 antibody (Alamone/Millipore). Although this reagent specifically detected KCNK3 via immunocytochemistry, it failed to detect a KCNK3-specific band by immunoblot in transfected HEK293 cells (not shown) and was therefore deemed unsuitable for use in biochemical studies. Thus, in order to perform biochemical studies, we transiently expressed HA-KCNK3 in HEK cells. Note that HA-KCNK3 has previously been shown to function identically to KCNK3 lacking the HA epitope tag (27). Under our lysis conditions, we detected both mature and immature KCNK3 species in total cell lysates, whereas only mature protein was detected in surface fractions (Fig. 3*A*). Under vehicle-treated conditions, 65.0 ± 6.9% of total KCNK3 was localized to the cell surface (Fig. 3*B*). Treatment with 1 μM PMA for 30 min at 37 °C significantly decreased KCNK3 surface levels to 47.4 ± 5.7% of total KCNK3 ($p < 0.04$; Student's *t* test; $n = 9$), which translated to a 27.1% loss in surface protein and is comparable with the current losses observed in both CGNs and HEK cells.

Because PKC-induced losses in KCNK3 activity mirrored surface losses of KCNK3 in HEK cells, we next determined whether the PKC-induced reduction in acid-sensitive leak current in CGNs was also due to rapid endocytosis. To detect native KCNK3 in primary CGNs, we raised rabbit antisera directed against the KCNK3 C terminus. This reagent specifically detected KCNK3 monomers in transfected HEK cells and CGNs (Fig. 3*C*). We used this reagent to determine whether the PKC-induced reduction in acid-sensitive leak current observed in CGNs was due to KCNK3 internalization. CGNs were treated with 1 μM PMA for 20 min at 37 °C, followed by cell surface biotinylation. Following vehicle treatment, we observed 5.0 ± 0.4% of total KCNK3 on the cell surface (Fig. 3*D*). Treatment with 1 μM PMA for 30 min at 37 °C significantly decreased KCNK3 surface levels to 3.74 ± 0.2% of total KCNK3 ($p < 0.04$, Student's *t* test; $n = 7$) (Fig. 3*D*). This translates to a 25.2% loss in surface KCNK3 protein, which is consistent with PMA-induced reduction of KCNK3 currents in HEK cells and acid-sensitive leak currents in CGNs.

We next used cellular imaging to examine KCNK3 cellular distribution in HEK cells. Under basal conditions, KCNK3 expressed prominently at the cell perimeter and co-localized with the IL2α receptor (Tac), co-expressed as a plasma membrane marker (38) (Fig. 4*A*). Following treatment with 1 μM PMA for 30 min at 37 °C, we observed a significant decrease in KCNK3 surface levels (Fig. 4*B*) and redistribution into intracellular puncta (Fig. 4, *A* and *C*), whereas Tac remained on the cell surface. PMA-induced losses from the cell surface were significantly blocked by pretreating cells with 1 μM BIM (Fig. 4*B*), demonstrating that PMA-induced losses were PKC-mediated. In order to test whether KCNK3 traffics via the endocytic pathway, we labeled endosomes with Alexa594-Tf during PMA-induced KCNK3 internalization. As seen in Fig. 4*C*, KCNK3 internalized into a subset of Tf-positive endosomes, suggesting that KCNK3 traffics via the endosomal pathway and, specifically, through Tf-positive endosomes. Following internalization, proteins can divert to either degradative or recycling endocytic pathways. To test whether KCNK3 is subject to degradation following internalization, we monitored KCNK3 stability over time with or without 1 μM PMA, following pretreatment with the translational inhibitor cycloheximide. KCNK3 was highly stable over a 60-min period, and PMA treatment had no effect on total KCNK3 protein levels (not shown), suggesting that following internalization, KCNK3 traffics through a non-deg-

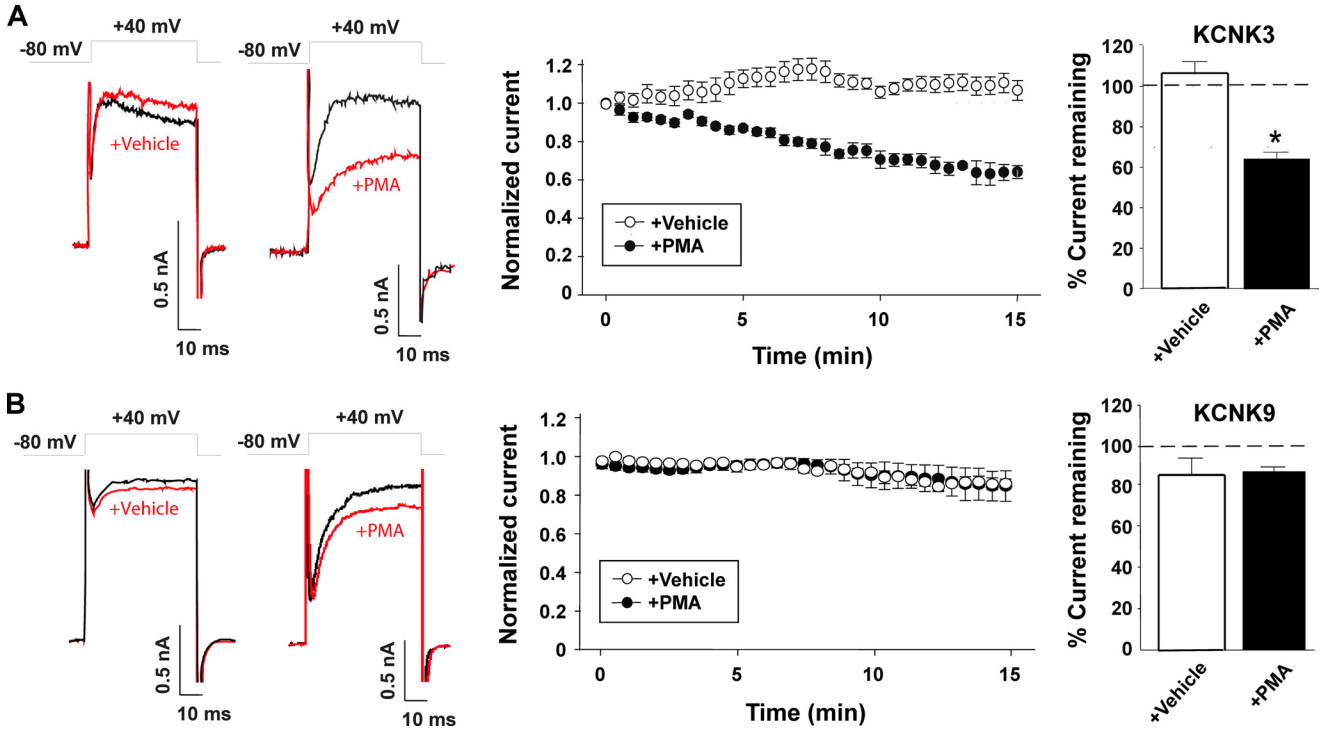

FIGURE 2. **PKC activation inhibits K^+ current in KCNK3- but not KCNK9-expressing HEK293T cells.** Whole-cell K^+ leak currents from cells expressing either KCNK3 (*A*) or KCNK9 (*B*) channels were induced using depolarizing voltage steps from −80 to +40 mV every 30 s. For the each channel, representative traces taken before (*black*) and at the end of 15 min treatment (*red*) with either vehicle (ethanol) or 1 μM PMA are shown on the *left*. Average normalized time courses of currents recorded during this treatment are shown in the *middle*. Mean ± S.E. (*error bars*) of normalized current inhibition (after a 15-min exposure to PMA) from several identical experiments is shown on the *right*. *, $p < 0.001$; Student's *t* test; $n = 3$–5.

radative pathway. Taken together, these data indicate that KCNK3 undergoes PKC-stimulated, non-degradative endocytosis.

Group I mGluR Activation Induces KCNK3 Down-regulation and Internalization—To investigate physiologically relevant stimuli that may regulate KCNK3 trafficking, we tested whether activating Group I mGluRs would alter KCNK3 function in CGNs. Group I mGluRs are abundantly expressed in CGNs (39, 40) and couple to G_q activation, which ultimately activates PKC. Moreover, Group I mGluR activation has been shown to decrease acid-sensitive currents in motor neurons (41). CGNs were treated with the Group I mGluR agonist DHPG (39, 42) (1 μM) during whole cell recording. We observed a rapid and significant reduction in leak currents (Fig. 5*A*) over 15 min in response to DHPG treatment (56 ± 10% current remaining; $n = 8$; $p < 0.01$) (Fig. 5*B*). Moreover, DHPG-mediated loss in current amplitude was significantly different from the small change ($p > 0.05$; not significant) in amplitude that occurred over 15 min with vehicle (94 ± 8% current remaining; $p < 0.02$; two-way *t* test for two means; $n = 7$). The DHPG-mediated decrease in current amplitude was comparable in magnitude with that observed following PMA treatment. To determine whether DHPG-mediated current losses were PKC-dependent, CGNs were pretreated with 1 μM BIM for at least 20 min at room temperature prior to DHPG application. BIM alone had no effect on acid-sensitive currents (107 ± 7.2% current remaining; $n = 4$ (not shown)) but completely blocked DHPG-mediated decreases in leak current (107 ± 27% current remaining; $n = 3$) (Fig. 5, *C–E*). In current recordings from the same groups of cells, DHPG significantly inhibited leak current over the 15-min time period (48.3 ± 11% current remaining; $p <$ 0.05; $n = 5$), demonstrating current sensitivity to Group I mGluR activation under these recording conditions. These results are consistent with PKC-mediated functional down-regulation of KCNK3 in response to Group I mGluR activation.

We next asked whether Group I mGluR activation stimulates KCNK3 internalization and, if so, whether mGluR-stimulated KCNK3 internalization is mediated by PKC. HEK cells were co-transfected with KCNK3 and a bicistronic vector expressing either GFP alone or GFP with mGluR5. Treatment with 1 μM DHPG for 20 min at 37 °C had no effect on KCNK3 surface levels in cells expressing KCNK3 and GFP ($p = 0.89$; Student's *t* test; $n = 6$) (Fig. 6*A*). In contrast, when KCNK3 was co-expressed with mGluR5, 1 μM DHPG treatment significantly decreased KCNK3 surface levels to 70.7 ± 5.0% of KCNK3 levels in vehicle-treated cells (Fig. 6*A*). mGluR5-mediated KCNK3 internalization required PKC activation because pretreatment with 1 μM BIM completely blocked mGluR5-mediated KCNK3 surface losses (Fig. 6*B*). Taken together, our results indicate that KCNK3 is acutely internalized in response to PKC activity associated with activation of Group I mGluR signaling.

KCNK3 C-terminal Residues Are both Necessary and Sufficient for PKC-regulated KCNK3 Internalization—We next sought to identify the molecular determinants of PKC-mediated KCNK3 internalization. We previously reported that the DAT encodes a novel C-terminal endocytic signal, FREKLAYAIA, that regulates both constitutive internalization and trafficking in response to PKC activation (36, 43, 44). KCNK3 encodes a homologous sequence, SREKLQYSIP, in C-terminal residues 334–343, which is absent in the KCNK3 homolog, KCNK9 (Fig. 7*A*). We used a gain-of-function assay to ask

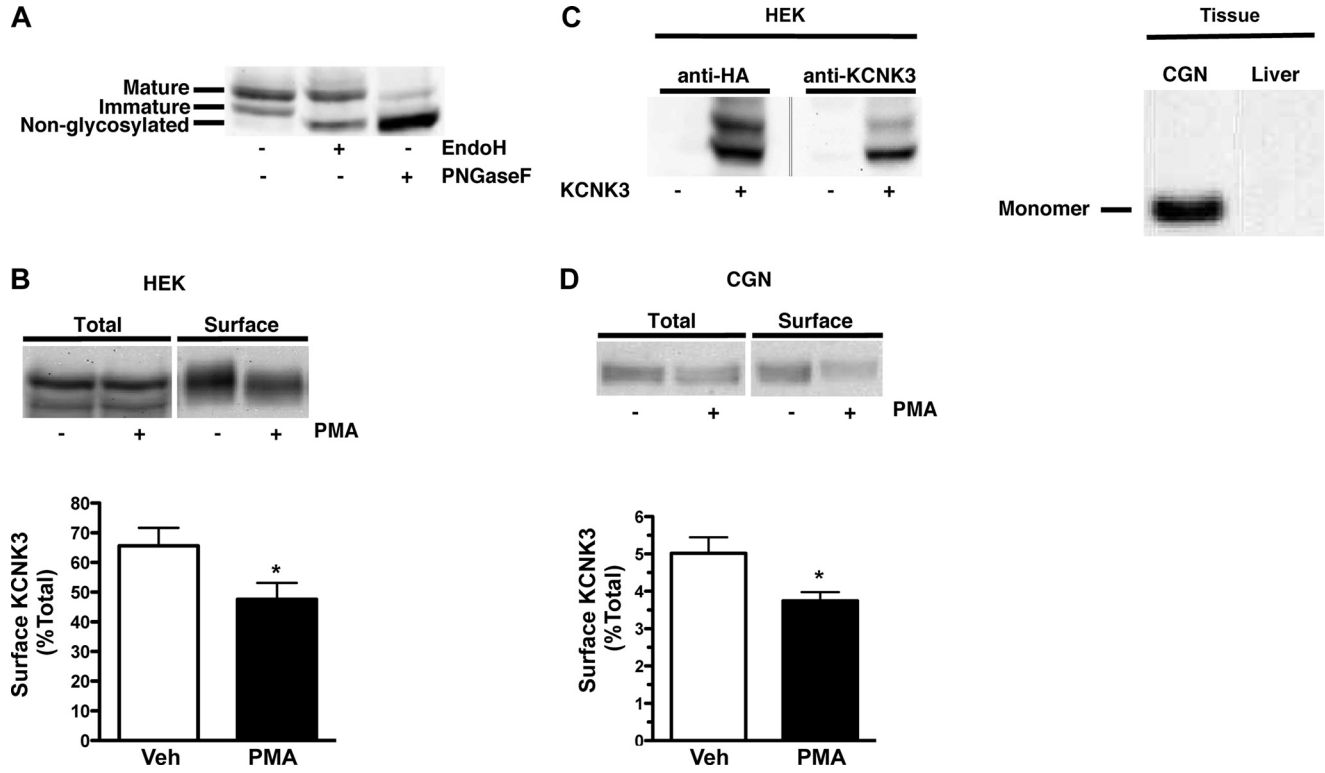

FIGURE 3. **PKC activation results in KCNK3 internalization via the endocytic pathway.** HEK cells were transfected with the indicated constructs and assayed 48 h post-transfection. CGNs were isolated as described under "Experimental Procedures." *A*, KCNK3 biosynthetic characterization. HEK293T cells were transfected with HA-KCNK3, and cell lysates were analyzed 48 h post-transfection. Lysates were treated with 1 unit of endoglycosidase H (*EndoH*) or peptide: *N*-glycosidase F (*PNGaseF*) for 3 h at 30 °C and resolved by SDS-PAGE, and immunoblots were probed using anti-HA antibody. Note detection of both KCNK3 mature (endoglycosidase H-insensitive) and immature (endoglycosidase H-sensitive) species. *B*, cell surface biotinylation. HEK cells transfected with HA-KCNK3 were treated or not treated with 1 μM PMA for 30 min at 37 °C, and KCNK3 surface levels were measured by biotinylation as described under "Experimental Procedures." *Top*, representative immunoblot showing total and surface KCNK3 protein detected with anti-HA antibody. *Bottom*, average data expressed as KCNK3 surface levels ± S.E. (*error bars*). *, significantly different from vehicle control; $p < 0.04$; Student's *t* test; $n = 9$. *C*, a C-terminal-directed rabbit anti-KCNK3 antibody specifically recognizes KCNK3 in transfected HEK cells. *Left*, HEK cells were transfected with either vector (−) or HA-KCNK3 (+), cell lysates were resolved by SDS-PAGE, and immunoblots were probed with anti-HA and rabbit anti-KCNK3 antibodies, in parallel. *Right*, the indicated tissues were harvested from P6 rat pups, lysed, and resolved by SDS-PAGE. Immunoblots with rabbit anti-KCNK3 antibody reveal specific KCNK3 immunoreactivity that is not present in the liver. *D*, cell surface biotinylation. CGNs were treated or not treated with 1 μM PMA for 30 min at 37 °C, and KCNK3 surface levels were measured by biotinylation as described under "Experimental Procedures." *Top*, representative immunoblot showing total and surface KCNK3 protein. *Bottom*, average KCNK3 surface levels expressed as a percentage of total KCNK3 ± S.E. *, significantly different from vehicle control; $p < 0.04$; Student's *t* test; $n = 7$.

whether the KCNK3 C terminus is sufficient to drive internalization of an endocytic-defective reporter protein, Tac. As seen in Fig. 7*B*, Tac was highly expressed at the cell surface under trafficking-restrictive conditions (4 °C), and remained at the surface in trafficking-permissive conditions (37 °C). In contrast, a Tac fusion protein expressing the KCNK3 C terminus robustly internalized at 37 °C. Internalization was specific to the KCNK3 C terminus because a Tac-KCNK9 fusion protein failed to internalize (Fig. 7*A*). These results indicate that the KCNK3 C terminus encodes residues sufficient to drive endocytosis, whereas the KCNK9 C terminus does not encode an endocytic determinant.

Given the sequence similarity between the DAT endocytic signal and the KCNK3 SREKLQYSIP residues, we next asked whether residues involved in PKC-regulated DAT internalization (36, 43) were also necessary for KCNK3 down-regulation and internalization. To test this possibility, we mutated KCNK3 residues 335–337 to alanines (REK/AAA) and tested the capacity of this mutant to undergo PKC-mediated down-regulation and internalization. The REK/AAA mutant expressed and exhibited whole cell currents comparable with those measured for the wild type channel (Fig. 7*B*). As observed previously, a 15-min treatment with 1 μM PMA resulted in significant, time-dependent decreases in wild type KCNK3 currents to 61.1 ± 7.6% of base-line levels (Fig. 7*B*). In contrast, the REK/AAA mutant was completely insensitive to PMA treatment, and no significant current losses were observed (97.6 ± 2.9% of base line) (Fig. 7*B*). To test whether KCNK3 residues 335–337 were required for PKC-induced KCNK3 internalization, we next used both cellular imaging and surface biotinylation to monitor KCNK3 REK/AAA endocytosis in response to PKC activation. Cellular imaging revealed that the REK/AAA mutant was expressed at the cell surface but failed to internalize following PKC activation for 15 min at 37 °C (Fig. 7*C*). Cell surface biotinylation (Fig. 7*D*) confirmed that mutating KCNK3 residues 335–337 significantly blocked PKC-mediated KCNK3 surface losses (wild type: 63.7 ± 7.5% of vehicle levels; REK/AAA: 114.4 ± 12.4% of vehicle levels, $p < 0.02$, Student's *t* test, $n = 4$), demonstrating that these three residues are key determinants of PKC-mediated KCNK3 functional down-regulation and internalization.

PKC-mediated KCNK3 Endocytosis Requires 14-3-3β—Previous studies have shown that the phosphoserine-binding protein 14-3-3β facilitates KCNK3 exit from the ER via an interac-

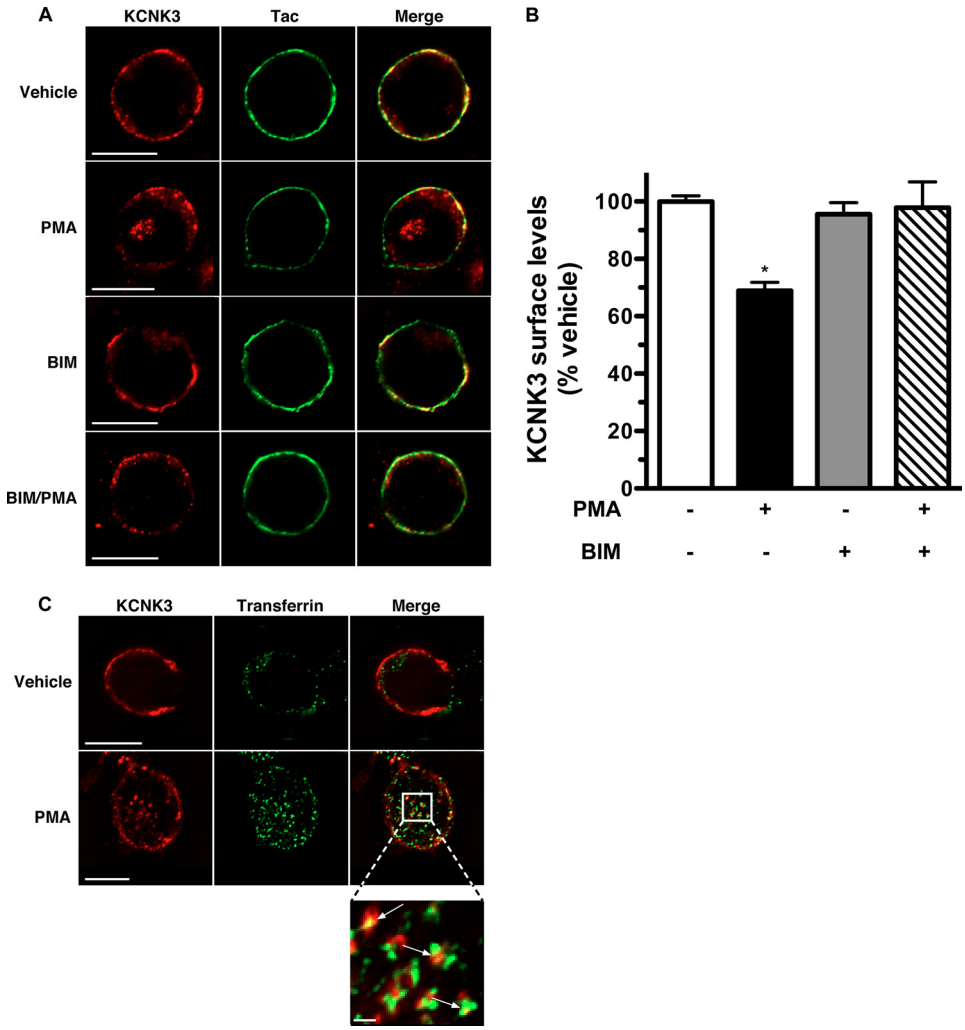

FIGURE 4. **KCNK3 internalizes into endocytic vesicles in a PKC-sensitive manner.** HEK cells were co-transfected with KCNK3 and the cell surface marker IL2αR (Tac) and were pretreated with or without 1 μM BIM, followed by treatment with or without 1 μM PMA for 30 min at 37 °C. Surface Tac was labeled on non-permeabilized cells with αTac antibody (*green*). Cells were then permeabilized and stained for KCNK3 (*red*). Images were captured and analyzed as described under "Experimental Procedures." *Scale bars*, 10 μm. *A*, representative images; *B*, image quantification. Data are expressed as percentage of vehicle surface levels ± S.E. (*error bars*). *, significantly different from vehicle, BIM, and BIM/PMA; $p < 0.05$; one-way analysis of variance with Tukey's multiple comparison test; $n = 12$. *C*, KCNK3 endocytic fate. Cells were treated or not treated with 1 μM PMA for 30 min at 37 °C in the presence of Alexa594-Tf (*green*), fixed, permeabilized, and stained for KCNK3 (*red*). *Scale bars*, 10 μm. *Enlarged view*, *scale bar*, 1 μm.

tion with the KCNK3 distal C terminus (27). However, we noticed that the SREKLQYSIP sequence is similar to the mode II 14-3-3 binding motif (R/K)$X\phi X$(pS/pT)XP (SREKLQYSIP), prompting us to ask whether 14-3-3β may play a role in PKC-mediated KCNK3 endocytosis. To test whether 14-3-3β is required for PKC-mediated KCNK3 internalization, we used a knockdown approach to limit 14-3-3β expression. Three shRNAs targeting human 14-3-3β were tested for their ability to decrease 14-3-3β expression levels. As seen in Fig. 8*A*, 14-3-3β shRNAs 6, 7, and 8 significantly decreased 14-3-3β levels 72 h post-transfection, as compared with vector-transfected controls, whereas a scrambled shRNA had no significant effect on 14-3-3β levels. Significant 14-3-3β knockdowns were also achieved 48 h post-transfection (not shown). HEK cells were co-transfected with KCNK3 and each of these shRNAs, and their ability to undergo PKC-stimulated internalization was assessed by cellular imaging following treatment with 1 μM PMA for 30 min at 37 °C. Under basal conditions, KCNK3 prominently localized to the cell surface, when co-expressed with either control 14-3-3β-directed shRNAs. PKC activation resulted in robust KCNK3 redistribution to intracellular puncta in cells co-expressing either GFP alone or GFP and scrambled shRNA (Fig. 8*B*). In contrast, KCNK3 failed to redistribute to intracellular puncta in cells co-expressing any of the three 14-3-3β-directed shRNAs (Fig. 8*B*). We further tested whether 14-3-3β was required for PKC-mediated functional down-regulation of KCNK3. Cells were co-transfected with GFP, scrambled shRNA, or 14-3-3β shRNA 7, and whole cell currents were recorded. As seen in Fig. 8*C*, application of 1 μM PMA significantly decreased KCNK3 currents in cells co-expressing either GFP (64.9 ± 5.6% of base line) or scrambled shRNA (74.9 ± 0.9% of base line). However, 14-3-3β-directed shRNA 7 significantly blocked the PMA-induced down-regulation of KCNK3 (91.8 ± 4.2% of base line). Taken together, these results indicate that 14-3-3β plays a requisite role in PKC-mediated KCNK3 internalization and implicates 14-3-3β in regulated endocytosis.

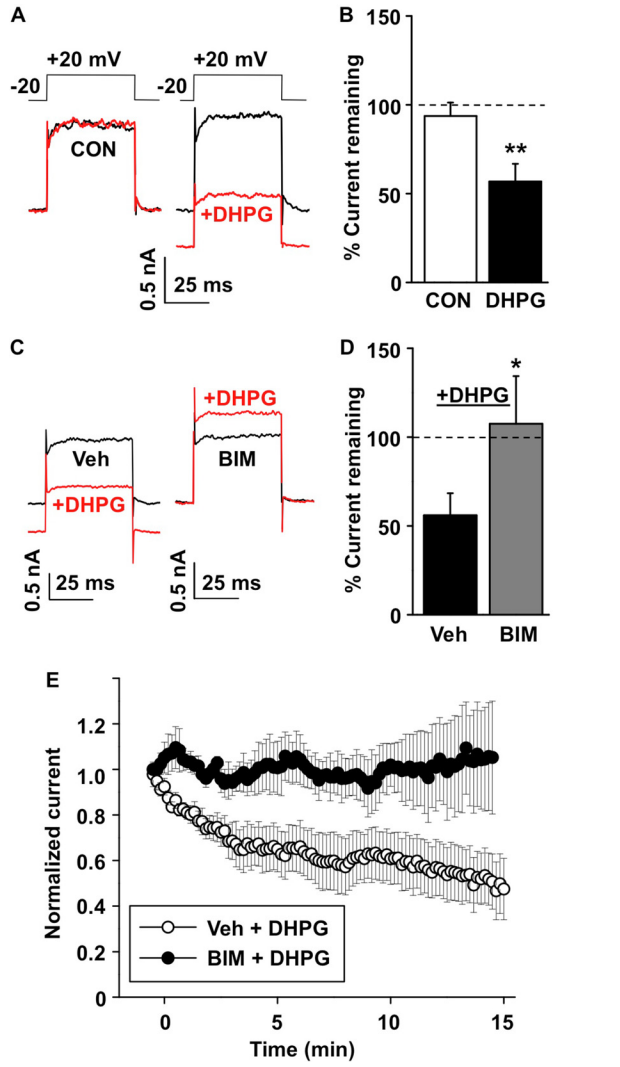

FIGURE 5. **Group I mGluR activation reduces leak current in CGNs**. Whole-cell recordings of K^+ leak current in the presence of 0.5 μM TTX and 10 mM TEA (7–14 days *in vitro*) were tested for sensitivity to the group I mGluR agonist DHPG. *A*, selected sweeps at time 0 min (*black line*) and 15 min (*red line*). *Left*, representative traces (*CON*) show leak current amplitude with no additions. *Right*, representative traces with and without 1 μM DHPG. *B*, average percentage of current remaining after 15 min of no additions (*CON*) or DHPG (n = 6–8/group). Cells exposed to DHPG exhibited significant inhibition of leak current compared with no addition (**, $p < 0.02$; two-way Student's t test for two means). *C*, *left*, cells were preincubated for at least 8 min in 0.005% DMSO (*Veh*) while recording whole-cell leak currents. Representative current traces *versus* time exhibit substantial decreases in amplitude after 15 min of 1 μM DHPG compared with time 0 min (*Veh*). *Right*, representative traces document that preincubating cells with 1 μM BIM for at least 8 min while in the whole-cell configuration minimized leak current inhibition by DHPG. *D*, average percentage of current remaining after 15 min of DHPG following preincubation with either 1 μM BIM (n = 3) or DMSO (*Veh*; n = 4). *, $p < 0.05$, compared with the presence of BIM using a two-way Student's t test for two means). *E*, time course of the average decrease in normalized leak currents over 15 min. DHPG was applied at time 0 min (n = 3–4/data point) in the presence of DMSO (○) or BIM (●). *Error bars*, S.E.

DISCUSSION

Membrane protein trafficking is a central mechanism controlling neuronal excitability and plasticity in the brain. Regulated internalization of ligand-gated ion channels, such as AMPA (45–47), NMDA (48–51) and $GABA_A$ (52, 53) receptors, is a key factor in synaptic plasticity. Recent studies indicate that endocytic trafficking acutely regulates several different types of K^+ channels, including K_{ATP} (54) and $K_{Ca.2.1}$ (55), suggesting that regulated membrane trafficking is a means to rapidly control K^+ channel density. Indeed, a recent study demonstrated that TWIK1 undergoes regulated internalization via a classic dileucine endocytic signal (56). In the current study, our data reveal that dynamic endocytic trafficking regulates acid-sensitive K^+ leak channel surface expression. This finding suggests a role for KCNK3 to uniquely contribute to synaptic plasticity. KCNK3 internalization would be predicted to depolarize the membrane potential, which would inactivate Na_v channels, causing the membrane to reach threshold more slowly, fail in firing, and/or spike at a slower frequency of bursting. Alternatively, membrane depolarization mediated by regulated KCNK3 trafficking could relieve Mg^{2+} block of NMDA receptors, increasing the probability of NMDA receptor firing and downstream plasticity events in response to an excitatory postsynaptic potential. Thus, in combination with established ligand-gated ion channel trafficking, acutely regulating KCNK3 surface levels would give rise to a multimodal, context-dependent plasticity of membrane excitability that could last for many minutes.

Prior studies using phorbol esters (31), Group I mGluR agonists (41), and M1/M3 muscarinic agonists (57, 58) demonstrated a PKC-mediated functional down-regulation of KCNK3 and/or acid-sensitive currents, respectively. However, the mechanisms underlying this down-regulation have not been well defined. We observed significant loss of KCNK3 activity in response to PMA treatment over a 15-min time course in both CGNs (Fig. 1) and HEK cells (Fig. 2), which is consistent with the time course for endocytosis. We used surface biotinylation and cellular imaging to directly test whether PKC-stimulated KCNK3 current losses were due to internalization. We observed significant PKC-dependent losses in surface KCNK3 following PMA treatment both in HEK cells (Fig. 3*B*) and CGNs (Fig. 3*D*), which were completely blocked by the PKC inhibitor BIM (Fig. 4, *A* and *B*). The magnitude of KCNK3 surface losses paralleled PKC-mediated KCNK3 currents losses, consistent with endocytosis as the primary mechanism responsible for PKC-mediated KCNK3 inhibition. Moreover, we observed losses in acid-sensitive leak currents (Fig. 5) and KCNK3 internalization (Fig. 6) via activation of endogenously expressed Group I mGluRs, consistent with previous reports demonstrating Group I mGluR-mediated KCNK3 down-regulation (41). Previous studies reported rapid KCNK3 activity losses in response to direct G_q activation (34) or via glutamatergic signaling (41, 59) in heterologous expression systems and CGNs, whereas we observed a slower time course of KCNK3 inhibition. These differences may be due to direct G_q activation in a heterologous expression system *versus* indirect via G_q coupling in our experiments. This difference may also reflect the much higher DHPG concentrations used in previous studies, compared with those used in our studies (10 and 100 μM *versus* 1 μM in our study). Indeed, decreased cAMP production in response to high DHPG concentrations has been reported (60), which is likely mediated by Group III mGluR activation. It is not known whether PKC activation results in KCNK3 phosphorylation, either directly or indirectly. A recent report demonstrated that endothelin-1 down-regulates KCNK3 and leads to PKC-depen-

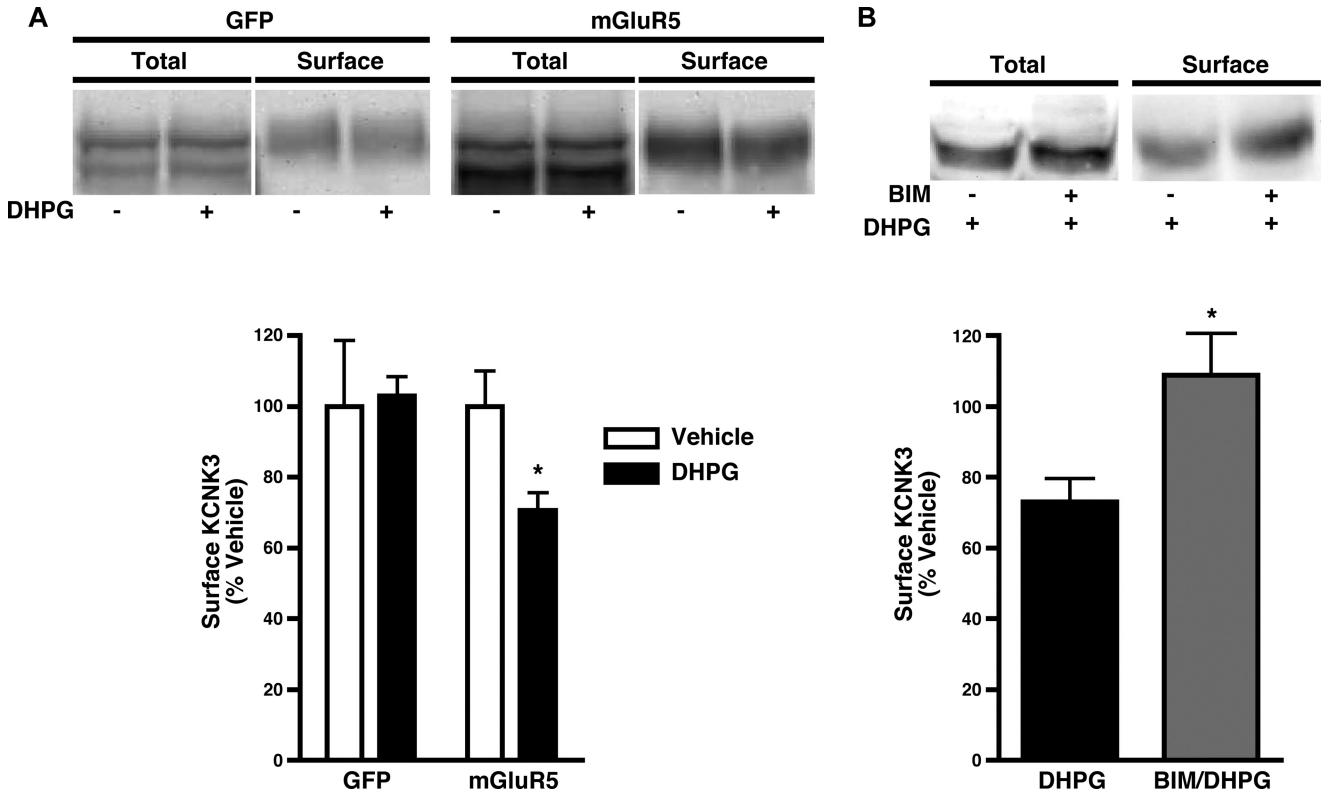

FIGURE 6. **mGluR5 activation stimulates PKC-dependent KCNK3 internalization.** *A*, cell surface biotinylation. Cells were treated or not treated with 1 μM DHPG for 20 min at 37 °C, and KCNK3 surface levels were measured as described under "Experimental Procedures." *Top*, representative immunoblot showing total and surface KCNK3 protein. *Bottom*, average KCNK3 surface levels expressed as percentage of vehicle ± S.E. (*error bars*). *, significantly different from vehicle control; $p < 0.03$; Student's *t* test; $n = 6$. *B*, cells were treated or not treated with 1 μM BIM for 20 min at 37 °C followed by treatment with or without 1 μM DHPG for 20 min at 37 °C, and KCNK3 surface levels were measured as described under "Experimental Procedures." *Top*, representative immunoblot showing KCNK3 total and surface protein. *Bottom*, average KCNK3 surface levels expressed as percentage of vehicle ± S.E. *, significantly different from vehicle control; $p < 0.03$; Student's *t* test; $n = 6$.

dent KCNK3 phosphorylation in pulmonary artery smooth muscle cells (61). However, it should be noted that these phosphorylation studies relied upon the commercially available anti-KCNK3 antibody that, in our hands, does not recognize a KNCK3-specific band (not shown). It is interesting to note that under basal conditions, KNCK3 surface expression in primary CGN cultures was <6% total KCNK3 protein, which differed markedly from observed surface levels in transfected HEK cells. Nevertheless, these values are consistent with those reported for other channels in both primary cultured neurons (62, 63) and acute brain slices (64). Low channel surface density (as a fraction of the total available channel) may reflect large intracellular endocytic pools tightly regulated by neuron-specific mechanisms. Alternatively, they may reflect a high degree of turnover in neuronal systems, with large, forward trafficking protein pools to maintain steady state channel levels in the membrane.

Following internalization from the cell surface, proteins can diverge to either recycling or degradative endocytic pathways (65). For example, EGFR (66, 67) and δ-opioid receptors (68) enter late endosomes and are degraded upon internalization, whereas the TfR is primarily recycled (65). We observed KCNK3 co-localization in an early endosome/TfR-positive vesicle population following internalization (Fig. 4*C*) and detected no losses in total KCNK3 protein following PKC stimulation (not shown). These results suggest that internalized KCNK3 is likely to enter a recycling, rather than a degradative, pathway.

Previous studies from our laboratory investigating mechanisms responsible for PKC-stimulated DAT trafficking revealed a novel endocytic regulatory domain (FREKLAYAIA) encoded in the DAT C terminus (36) that is highly conserved across the SLC6 transporter gene family and is the locus for an endocytic braking mechanism (43). Sequence comparison across the mammalian genome revealed that KCNK3 is the only membrane protein outside of the SLC6 transporter gene family to encode a homologous endocytic signal. Gain-of-function assays revealed that the KCNK3 C terminus is sufficient for endocytosis (Fig. 7*A*), and that the REK residues are absolutely required for PKC-mediated KCNK3 down-regulation and internalization (Fig. 7, *B–D*). These results offer further insight into the previous results of Tally and Bayliss (19), in which KCNK3 C-terminal deletions that encompassed the 335–344 region abolished TRH receptor-mediated KCNK3 inhibition, which also occurs via G_q activation (69). It is currently not clear how these charged residues function to target either DAT or KCNK3 to the endocytic machinery. Answers to this question await future studies.

PKC-stimulated KCNK3 endocytosis absolutely required the phosphoserine-binding protein 14-3-3β. 14-3-3β belongs to the family of 14-3-3 phosphoserine-binding proteins, which are widely expressed in the brain and periphery and exist as homo- or heterodimers (70, 71). 14-3-3 binds target proteins primarily at either RS*X*pS*X*P or (R/K)*X*ϕ*X*(pS/pT)*X*P motifs (72, 73), and

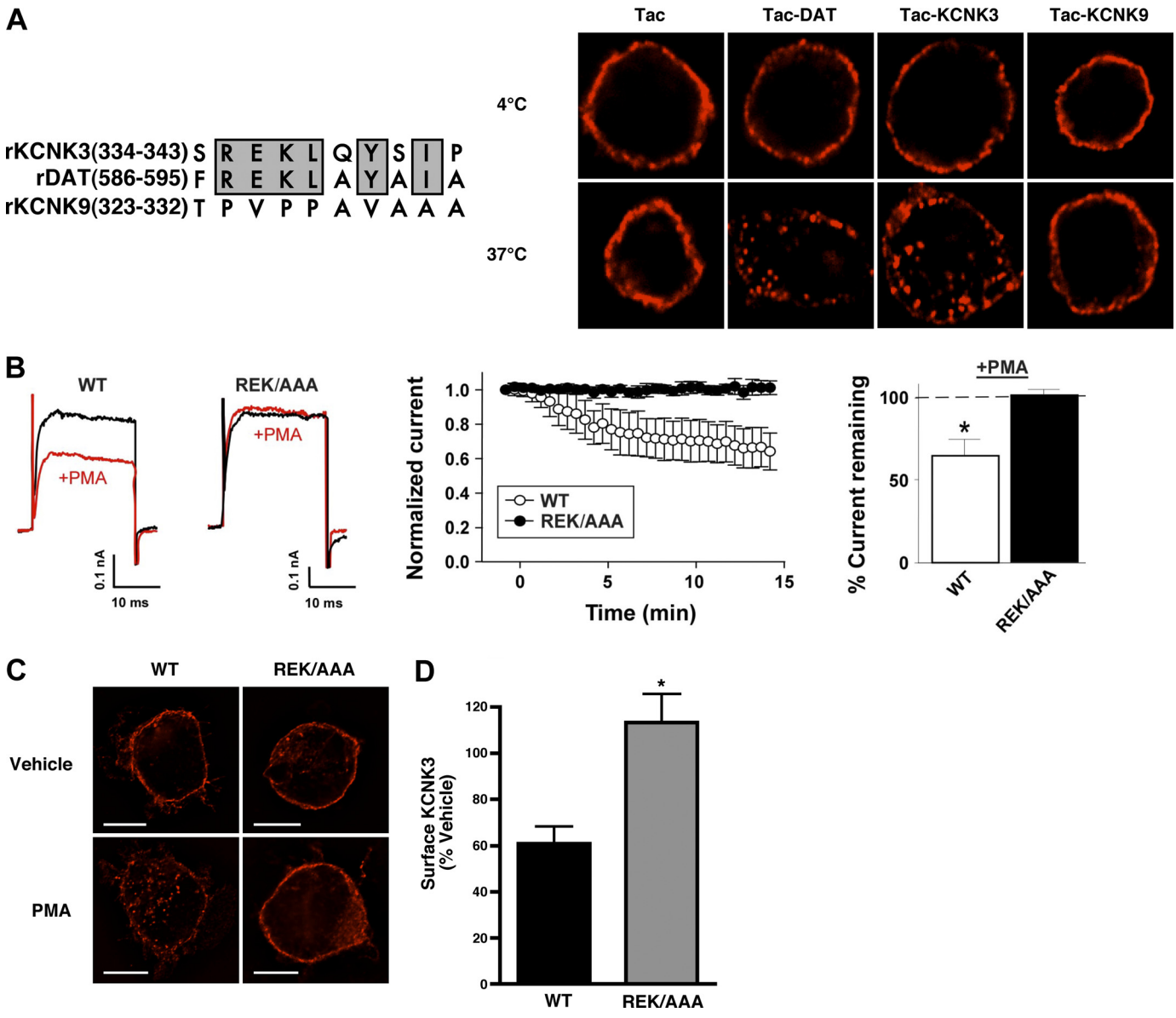

FIGURE 7. **KCNK3 encodes a PKC-sensitive endocytic signal at C-terminal residues 335–337.** PC12 (*A*) and HEK cells (*B–D*) were transfected with the indicated constructs and assayed 24–48 h post-transfection. *A*, *left*, sequence alignment between DAT and the potassium channel KCNK3 and KCNK9 C-terminal subregions. *Right*, immunocytochemistry. Intact cells were incubated in αTac antibody at 4 °C, shifted to 37 °C for 30 min, and then fixed and imaged as described under "Experimental Procedures." *B*, the REK/AAA mutation prevents PMA-induced inhibition of KCNK3 current. *Left*, representative traces of KCNK3 current recorded from HEK293T cells expressing either WT or REK/AAA mutant channels recorded before (*black*) and after (*red*) 1 μM PMA treatment (40-mV test pulse). *Middle*, average normalized time course of WT (*open circles*; $n = 3$) or REK/AAA (*filled circles*; $n = 5$) currents recorded during a 15-min exposure to 1 μM PMA. *Right*, mean ± S.E. of current remaining after a 15-min exposure to PMA ($p = 0.007$). *C*, immunocytochemistry. Cells were treated or not treated with 1 μM PMA for 30 min at 37 °C, fixed, stained for KCNK3, and imaged as described under "Experimental Procedures." *Scale bars*, 10 μm. *D*, cell surface biotinylation. Cells were treated or not treated with 1 μM PMA for 15 min at 37 °C, and KCNK3 surface levels were measured as described under "Experimental Procedures." Average KCNK3 surface levels following PMA treatment are expressed as percentage of vehicle ± S.E. (*error bars*). *, significantly different from WT; $p < 0.02$; Student's *t* test; $n = 4$.

several proteins encode multiple 14-3-3 binding sites (74, 75). 14-3-3 binding can 1) induce conformation changes that facilitate catalytic activity or protein-protein interactions, 2) mask domains to prevent protein-protein interactions, or 3) facilitate protein co-localization. Previous work demonstrated that 14-3-3β binds to a non-canonical 14-3-3 binding motif in the distal KCNK3 C terminus and is required for KCNK3 egress from the ER (27, 28, 76). In addition, other 14-3-3 isoforms can interact with the KCNK3 C terminus and promote increased KCNK3 surface density (77); however, it is not clear whether the increased KCNK3 surface expression is due to ER egress or endocytic trafficking. Our results indicate that 14-3-3β is also necessary for PKC-mediated KNCK3 internalization. We noted that a ~50% 14-3-3β knockdown did not markedly disrupt KCNK3 surface targeting, whereas PKC-mediated endocytosis was abolished (Fig. 8). This may suggest that forward trafficking from the ER is less sensitive to 14-3-3β levels than KCNK3 surface populations. Alternatively, other accessory proteins working in consort with 14-3-3β at the cell surface may be expressed in limited quantities and are thereby more sensitive to losses in 14-3-3β. Interestingly, the epithelial sodium channel, ENaC, constitutively internalizes in a 14-3-3- and Nedd4-

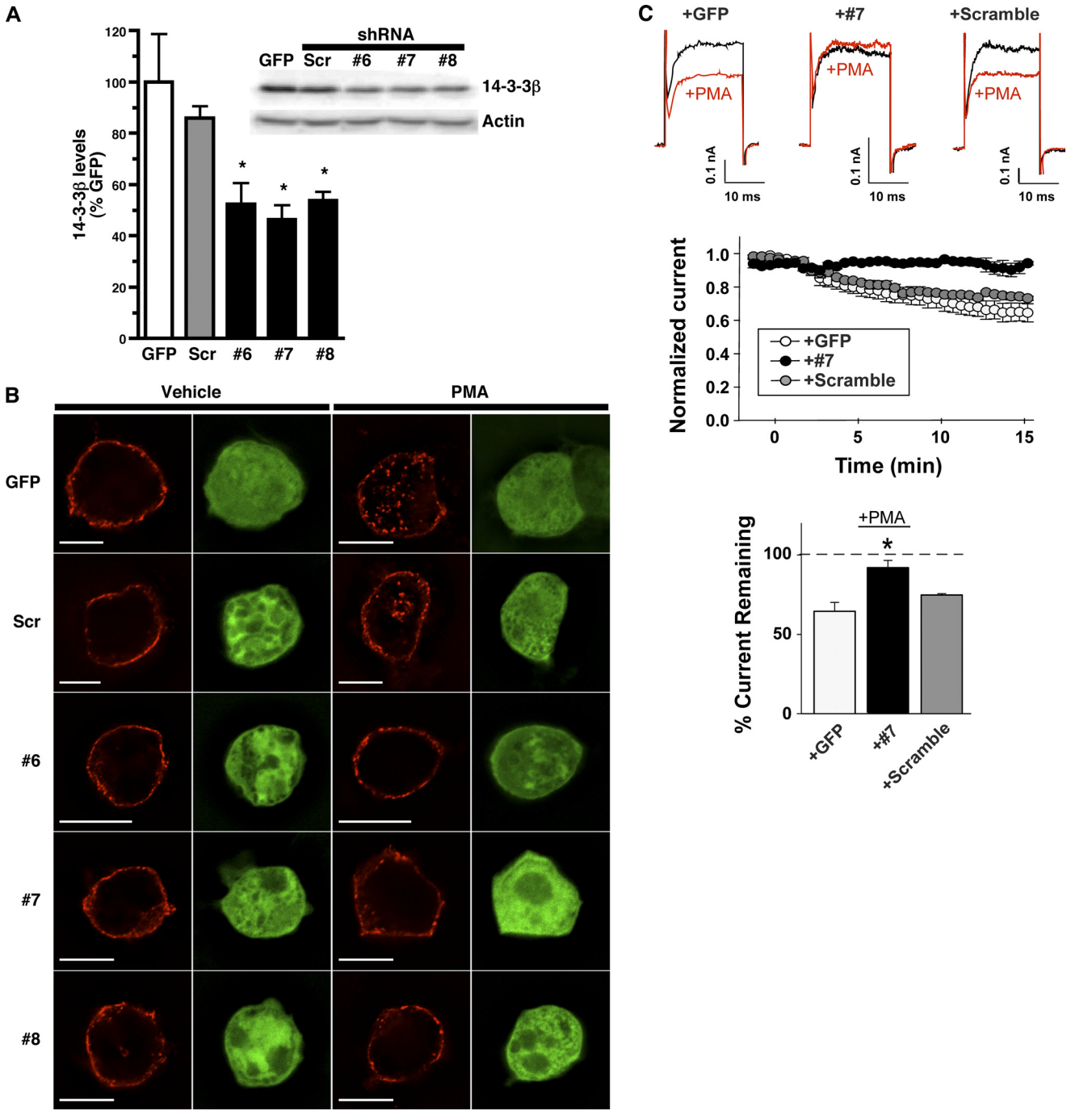

FIGURE 8. **PKC-stimulated KCNK3 internalization requires 14-3-3β.** HEK cells were transfected with the indicated constructs and assayed 48 h (*A* and *D*) or 72 h (*B* and *C*) post-transfection. *A*, shRNA-mediated 14-3-3β knockdown. Average 14-3-3β protein levels are expressed as percentage of control levels ± S.E. *, significantly different from GFP-transfected controls; $p < 0.004$; one-way analysis of variance with Dunnett's post hoc analysis; $n = 4$. *Inset*, representative immunoblot probed for 14-3-3β and actin (loading control). *B*, immunocytochemistry. Cells were treated or not treated with 1 μM PMA for 30 min at 37 °C, fixed, and stained for KCNK3 (*red*). GFP expression indicates shRNA co-transfection (*green*). Images were captured and analyzed as described under "Experimental Procedures." *Scale bars*, 10 μm. *C*, PKC-mediated inhibition of KCNK3 current requires 14-3-3β. *Top*, representative whole-cell current traces from HEK293T cells co-expressing KCNK3 with either GFP, shRNA 7, or scrambled shRNA recorded before (*black*) and after (*red*) 1 μM PMA treatment (40-mV test pulse). Average normalized time course (*middle*) and mean ± S.E. (*error bars*) of current remaining (*bottom*) after 15 min of PMA treatment are shown; $n = 9$ for GFP control; $n = 4$ for scrambled and number 7 shRNAs. *Significantly different from wildtype, $p < .02$, one-way ANOVA with Bonferroni's multiple comparison test.

2-dependent manner, and aldosterone increases ENaC surface expression via blocking 14-3-3-dependent ENaC internalization and degradation (78–80). The mechanism by which 14-3-3β promotes KCNK3 internalization is not known; nor is it clear whether a mechanism distinct from 14-3-3β-dependent ER exit is at play. It is interesting to note that the SREKLQYSIP region is similar to the mode II 14-3-3β binding motif (R/K)$X\phi X$(pS/pT)XP (72, 73). Although we do not currently know whether 14-3-3β controls KCNK3 internalization directly or indirectly, this site is a candidate locus for potential 14-3-3β/KCNK3 endocytic interactions, distinct from the identified sequence controlling KCNK3 egress from the ER (27,

28). Future studies exploring the possibility of this sequence as a *bona fide* 14-3-3β binding site should be illuminating.

In summary, our results reveal that KCNK3 is subject to dynamic PKC-regulated endocytic trafficking that is 14-3-3β-dependent. This extends the physiological repertoire for 14-3-3β to now include neuronal endocytic trafficking. Moreover, given the central role of KCNK3 in maintaining the neuronal resting membrane potential, regulated KCNK3 trafficking holds the potential for a role for KCNK3 in synaptic plasticity.

REFERENCES

1. Johnston, J., Forsythe, I. D., and Kopp-Scheinpflug, C. (2010) Going native. Voltage-gated potassium channels controlling neuronal excitability. *J. Physiol.* **588,** 3187–3200
2. Dodson, P. D., and Forsythe, I. D. (2004) Presynaptic K^+ channels. Electrifying regulators of synaptic terminal excitability. *Trends Neurosci.* **27,** 210–217
3. Mathie, A., Al-Moubarak, E., and Veale, E. L. (2010) Gating of two-pore domain potassium channels. *J. Physiol.* **588,** 3149–3156
4. Enyedi, P., and Czirják, G. (2010) Molecular background of leak K^+ currents. Two-pore domain potassium channels. *Physiol. Rev.* **90,** 559–605
5. Buckingham, S. D., Kidd, J. F., Law, R. J., Franks, C. J., and Sattelle, D. B. (2005) Structure and function of two-pore domain K^+ channels. Contributions from genetic model organisms. *Trends Pharmacol. Sci.* **26,** 361–367
6. Bayliss, D. A., Sirois, J. E., and Talley, E. M. (2003) The TASK family. Two-pore domain background K^+ channels. *Mol. Interv.* **3,** 205–219
7. Goldstein, S. A., Wang, K. W., Ilan, N., and Pausch, M. H. (1998) Sequence and function of the two P domain potassium channels. Implications of an emerging superfamily. *J. Mol. Med.* **76,** 13–20
8. Ahern, C. A., and Kobertz, W. R. (2009) Chemical tools for K^+ channel biology. *Biochemistry* **48,** 517–526
9. Gouaux, E., and Mackinnon, R. (2005) Principles of selective ion transport in channels and pumps. *Science* **310,** 1461–1465
10. Talley, E. M., Solorzano, G., Lei, Q., Kim, D., and Bayliss, D. A. (2001) Cns distribution of members of the two-pore domain (KCNK) potassium channel family. *J. Neurosci.* **21,** 7491–7505
11. Millar, J. A., Barratt, L., Southan, A. P., Page, K. M., Fyffe, R. E., Robertson, B., and Mathie, A. (2000) A functional role for the two-pore domain potassium channel TASK-1 in cerebellar granule neurons. *Proc. Natl. Acad. Sci. U.S.A.* **97,** 3614–3618
12. Bayliss, D. A., Talley, E. M., Sirois, J. E., and Lei, Q. (2001) TASK-1 is a highly modulated pH-sensitive "leak" K^+ channel expressed in brainstem respiratory neurons. *Respir. Physiol.* **129,** 159–174
13. Czirják, G., and Enyedi, P. (2002) Formation of functional heterodimers between the TASK-1 and TASK-3 two-pore domain potassium channel subunits. *J. Biol. Chem.* **277,** 5426–5432
14. Berg, A. P., Talley, E. M., Manger, J. P., and Bayliss, D. A. (2004) Motoneurons express heteromeric TWIK-related acid-sensitive K^+ (TASK) channels containing TASK-1 (KCNK3) and TASK-3 (KCNK9) subunits. *J. Neurosci.* **24,** 6693–6702
15. Kang, D., Han, J., Talley, E. M., Bayliss, D. A., and Kim, D. (2004) Functional expression of TASK-1/TASK-3 heteromers in cerebellar granule cells. *J. Physiol.* **554,** 64–77
16. Lesage, F., and Lazdunski, M. (2000) Molecular and functional properties of two-pore domain potassium channels. *Am. J. Physiol. Renal Physiol.* **279,** F793–F801
17. Gruss, M., Bushell, T. J., Bright, D. P., Lieb, W. R., Mathie, A., and Franks, N. P. (2004) Two-pore domain K^+ channels are a novel target for the anesthetic gases xenon, nitrous oxide, and cyclopropane. *Mol. Pharmacol.* **65,** 443–452
18. Sirois, J. E., Lei, Q., Talley, E. M., Lynch, C., 3rd, and Bayliss, D. A. (2000) The TASK-1 two-pore domain K^+ channel is a molecular substrate for neuronal effects of inhalation anesthetics. *J. Neurosci.* **20,** 6347–6354
19. Talley, E. M., and Bayliss, D. A. (2002) Modulation of TASK-1 (Kcnk3) and TASK-3 (Kcnk9) potassium channels. Volatile anesthetics and neurotransmitters share a molecular site of action. *J. Biol. Chem.* **277,** 17733–17742
20. Putzke, C., Hanley, P. J., Schlichthörl, G., Preisig-Müller, R., Rinné, S., Anetseder, M., Eckenhoff, R., Berkowitz, C., Vassiliou, T., Wulf, H., and Eberhart, L. (2007) Differential effects of volatile and intravenous anesthetics on the activity of human TASK-1. *Am. J. Physiol. Cell Physiol.* **293,** C1319–C1326
21. Kindler, C. H., and Yost, C. S. (2005) Two-pore domain potassium channels. New sites of local anesthetic action and toxicity. *Reg. Anesth. Pain Med.* **30,** 260–274
22. Bautista, D. M., Sigal, Y. M., Milstein, A. D., Garrison, J. L., Zorn, J. A., Tsuruda, P. R., Nicoll, R. A., and Julius, D. (2008) Pungent agents from Szechuan peppers excite sensory neurons by inhibiting two-pore potassium channels. *Nat. Neurosci.* **11,** 772–779
23. Meuth, S. G., Kleinschnitz, C., Broicher, T., Austinat, M., Braeuninger, S., Bittner, S., Fischer, S., Bayliss, D. A., Budde, T., Stoll, G., and Wiendl, H. (2009) The neuroprotective impact of the leak potassium channel TASK1 on stroke development in mice. *Neurobiol. Dis.* **33,** 1–11
24. Trapp, S., Aller, M. I., Wisden, W., and Gourine, A. V. (2008) A role for TASK-1 (KCNK3) channels in the chemosensory control of breathing. *J. Neurosci.* **28,** 8844–8850
25. Davies, L. A., Hu, C., Guagliardo, N. A., Sen, N., Chen, X., Talley, E. M., Carey, R. M., Bayliss, D. A., and Barrett, P. Q. (2008) TASK channel deletion in mice causes primary hyperaldosteronism. *Proc. Natl. Acad. Sci. U.S.A.* **105,** 2203–2208
26. Mant, A., Elliott, D., Eyers, P. A., and O'Kelly, I. M. (2011) Protein kinase A is central for forward transport of two-pore domain potassium channels K2P3.1 and K2P9.1. *J. Biol. Chem.* **286,** 14110–14119
27. O'Kelly, I., Butler, M. H., Zilberberg, N., and Goldstein, S. A. (2002) Forward transport. 14-3-3 binding overcomes retention in endoplasmic reticulum by dibasic signals. *Cell* **111,** 577–588
28. O'Kelly, I., and Goldstein, S. A. (2008) Forward transport of K2p3.1. Mediation by 14-3-3 and COPI, modulation by p11. *Traffic* **9,** 72–78
29. Girard, C., Tinel, N., Terrenoire, C., Romey, G., Lazdunski, M., and Borsotto, M. (2002) p11, an annexin II subunit, an auxiliary protein associated with the background K^+ channel, TASK-1. *EMBO J.* **21,** 4439–4448
30. Renigunta, V., Yuan, H., Zuzarte, M., Rinné, S., Koch, A., Wischmeyer, E., Schlichthörl, G., Gao, Y., Karschin, A., Jacob, R., Schwappach, B., Daut, J., and Preisig-Müller, R. (2006) The retention factor p11 confers an endoplasmic reticulum localization signal to the potassium channel TASK-1. *Traffic* **7,** 168–181
31. Lopes, C. M., Gallagher, P. G., Buck, M. E., Butler, M. H., and Goldstein, S. A. (2000) Proton block and voltage gating are potassium-dependent in the cardiac leak channel Kcnk3. *J. Biol. Chem.* **275,** 16969–16978
32. Mathie, A. (2007) Neuronal two-pore domain potassium channels and their regulation by G protein-coupled receptors. *J. Physiol.* **578,** 377–385
33. Veale, E. L., Kennard, L. E., Sutton, G. L., MacKenzie, G., Sandu, C., and Mathie, A. (2007) Gα_q-mediated regulation of TASK3 two-pore domain potassium channels. The role of protein kinase C. *Mol. Pharmacol.* **71,** 1666–1675
34. Chen, X., Talley, E. M., Patel, N., Gomis, A., McIntire, W. E., Dong, B., Viana, F., Garrison, J. C., and Bayliss, D. A. (2006) Inhibition of a background potassium channel by G_q protein α-subunits. *Proc. Natl. Acad. Sci. U.S.A.* **103,** 3422–3427
35. Loder, M. K., and Melikian, H. E. (2003) The dopamine transporter constitutively internalizes and recycles in a protein kinase C-regulated manner in stably transfected PC12 cell lines. *J. Biol. Chem.* **278,** 22168–22174
36. Holton, K. L., Loder, M. K., and Melikian, H. E. (2005) Nonclassical, distinct endocytic signals dictate constitutive and PKC-regulated neurotransmitter transporter internalization. *Nat. Neurosci.* **8,** 881–888
37. Besana, A., Barbuti, A., Tateyama, M. A., Symes, A. J., Robinson, R. B., and Feinmark, S. J. (2004) Activation of protein kinase C epsilon inhibits the two-pore domain K^+ channel, TASK-1, inducing repolarization abnormalities in cardiac ventricular myocytes. *J. Biol. Chem.* **279,** 33154–33160
38. Tan, P. K., Waites, C., Liu, Y., Krantz, D. E., and Edwards, R. H. (1998) A leucine-based motif mediates the endocytosis of vesicular monoamine and acetylcholine transporters. *J. Biol. Chem.* **273,** 17351–17360
39. Niswender, C. M., and Conn, P. J. (2010) Metabotropic glutamate recep-

tors. Physiology, pharmacology, and disease. *Annu. Rev. Pharmacol. Toxicol.* **50,** 295–322
40. Prézeau, L., Carrette, J., Helpap, B., Curry, K., Pin, J. P., and Bockaert, J. (1994) Pharmacological characterization of metabotropic glutamate receptors in several types of brain cells in primary cultures. *Mol. Pharmacol.* **45,** 570–577
41. Talley, E. M., Lei, Q., Sirois, J. E., and Bayliss, D. A. (2000) TASK-1, a two-pore domain K^+ channel, is modulated by multiple neurotransmitters in motoneurons. *Neuron* **25,** 399–410
42. Ritzén, A., Mathiesen, J. M., and Thomsen, C. (2005) Molecular pharmacology and therapeutic prospects of metabotropic glutamate receptor allosteric modulators. *Basic Clin. Pharmacol. Toxicol.* **97,** 202–213
43. Boudanova, E., Navaroli, D. M., Stevens, Z., and Melikian, H. E. (2008) Dopamine transporter endocytic determinants. Carboxyl-terminal residues critical for basal and PKC-stimulated internalization. *Mol. Cell Neurosci.* **39,** 211–217
44. Navaroli, D. M., Stevens, Z. H., Uzelac, Z., Gabriel, L., King, M. J., Lifshitz, L. M., Sitte, H. H., and Melikian, H. E. (2011) The plasma membrane-associated GTPase Rin interacts with the dopamine transporter and is required for protein kinase C-regulated dopamine transporter trafficking. *J. Neurosci.* **31,** 13758–13770
45. Derkach, V. A., Oh, M. C., Guire, E. S., and Soderling, T. R. (2007) Regulatory mechanisms of AMPA receptors in synaptic plasticity. *Nat. Rev. Neurosci.* **8,** 101–113
46. Malenka, R. C. (2003) Synaptic plasticity and AMPA receptor trafficking. *Ann. N.Y. Acad. Sci.* **1003,** 1–11
47. Bredt, D. S., and Nicoll, R. A. (2003) AMPA receptor trafficking at excitatory synapses. *Neuron* **40,** 361–379
48. Lau, C. G., and Zukin, R. S. (2007) NMDA receptor trafficking in synaptic plasticity and neuropsychiatric disorders. *Nat. Rev. Neurosci.* **8,** 413–426
49. Groc, L., and Choquet, D. (2006) AMPA and NMDA glutamate receptor trafficking. Multiple roads for reaching and leaving the synapse. *Cell Tissue Res.* **326,** 423–438
50. Pérez-Otaño, I., and Ehlers, M. D. (2005) Homeostatic plasticity and NMDA receptor trafficking. *Trends Neurosci.* **28,** 229–238
51. Carroll, R. C., and Zukin, R. S. (2002) NMDA receptor trafficking and targeting. Implications for synaptic transmission and plasticity. *Trends Neurosci.* **25,** 571–577
52. Collingridge, G. L., Isaac, J. T., and Wang, Y. T. (2004) Receptor trafficking and synaptic plasticity. *Nat. Rev. Neurosci.* **5,** 952–962
53. Kittler, J. T., McAinsh, K., and Moss, S. J. (2002) Mechanisms of GABAA receptor assembly and trafficking. Implications for the modulation of inhibitory neurotransmission. *Mol. Neurobiol.* **26,** 251–268
54. Manna, P. T., Smith, A. J., Taneja, T. K., Howell, G. J., Lippiat, J. D., and Sivaprasadarao, A. (2010) Constitutive endocytic recycling and protein kinase C-mediated lysosomal degradation control K_{ATP} channel surface density. *J. Biol. Chem.* **285,** 5963–5973
55. Corrêa, S. A., Müller, J., Collingridge, G. L., and Marrion, N. V. (2009) Rapid endocytosis provides restricted somatic expression of a K^+ channel in central neurons. *J. Cell Sci.* **122,** 4186–4194
56. Feliciangeli, S., Tardy, M. P., Sandoz, G., Chatelain, F. C., Warth, R., Barhanin, J., Bendahhou, S., and Lesage, F. (2010) Potassium channel silencing by constitutive endocytosis and intracellular sequestration. *J. Biol. Chem.* **285,** 4798–4805
57. Meuth, S. G., Budde, T., Kanyshkova, T., Broicher, T., Munsch, T., and Pape, H. C. (2003) Contribution of TWIK-related acid-sensitive K^+ channel 1 (TASK1) and TASK3 channels to the control of activity modes in thalamocortical neurons. *J. Neurosci.* **23,** 6460–6469
58. Inoue, M., Harada, K., Matsuoka, H., Sata, T., and Warashina, A. (2008) Inhibition of TASK1-like channels by muscarinic receptor stimulation in rat adrenal medullary cells. *J. Neurochem.* **106,** 1804–1814
59. Chemin, J., Girard, C., Duprat, F., Lesage, F., Romey, G., and Lazdunski, M. (2003) Mechanisms underlying excitatory effects of group I metabotropic glutamate receptors via inhibition of 2P domain K^+ channels. *EMBO J.* **22,** 5403–5411
60. Sekiyama, N., Hayashi, Y., Nakanishi, S., Jane, D. E., Tse, H. W., Birse, E. F., and Watkins, J. C. (1996) Structure-activity relationships of new agonists and antagonists of different metabotropic glutamate receptor subtypes. *Br. J. Pharmacol.* **117,** 1493–1503
61. Tang, B., Li, Y., Nagaraj, C., Morty, R. E., Gabor, S., Stacher, E., Voswinckel, R., Weissmann, N., Leithner, K., Olschewski, H., and Olschewski, A. (2009) Endothelin-1 inhibits background two-pore domain channel TASK-1 in primary human pulmonary artery smooth muscle cells. *Am. J. Respir. Cell Mol. Biol.* **41,** 476–483
62. Gross, C., Yao, X., Pong, D. L., Jeromin, A., and Bassell, G. J. (2011) Fragile X mental retardation protein regulates protein expression and mRNA translation of the potassium channel Kv4.2. *J. Neurosci.* **31,** 5693–5698
63. Noam, Y., Zha, Q., Phan, L., Wu, R. L., Chetkovich, D. M., Wadman, W. J., and Baram, T. Z. (2010) Trafficking and surface expression of hyperpolarization-activated cyclic nucleotide-gated channels in hippocampal neurons. *J. Biol. Chem.* **285,** 14724–14736
64. Kim, D. Y., Gersbacher, M. T., Inquimbert, P., and Kovacs, D. M. (2011) Reduced sodium channel $Na_v1.1$ levels in BACE1-null mice. *J. Biol. Chem.* **286,** 8106–8116
65. Bonifacino, J. S., and Traub, L. M. (2003) Signals for sorting of transmembrane proteins to endosomes and lysosomes. *Annu. Rev. Biochem.* **72,** 395–447
66. Avraham, R., and Yarden, Y. (2011) Feedback regulation of EGFR signaling. Decision making by early and delayed loops. *Nat. Rev. Mol. Cell Biol.* **12,** 104–117
67. Huang, F., Kirkpatrick, D., Jiang, X., Gygi, S., and Sorkin, A. (2006) Differential regulation of EGF receptor internalization and degradation by multiubiquitination within the kinase domain. *Mol. Cell* **21,** 737–748
68. von Zastrow, M. (2010) Regulation of opioid receptors by endocytic membrane traffic. Mechanisms and translational implications. *Drug Alcohol Depend.* **108,** 166–171
69. Smith, J., Yu, R., and Hinkle, P. M. (2001) Activation of MAPK by TRH requires clathrin-dependent endocytosis and PKC but not receptor interaction with β-arrestin or receptor endocytosis. *Mol. Endocrinol.* **15,** 1539–1548
70. Bridges, D., and Moorhead, G. B. (2005) *Sci. STKE* **2005,** re10
71. Obsilová, V., Silhan, J., Boura, E., Teisinger, J., and Obsil, T. (2008) 14-3-3 proteins. A family of versatile molecular regulators. *Physiol. Res.* **57,** S11–S21
72. Yaffe, M. B., Rittinger, K., Volinia, S., Caron, P. R., Aitken, A., Leffers, H., Gamblin, S. J., Smerdon, S. J., and Cantley, L. C. (1997) The structural basis for 14-3-3-phosphopeptide binding specificity. *Cell* **91,** 961–971
73. Muslin, A. J., Tanner, J. W., Allen, P. M., and Shaw, A. S. (1996) Interaction of 14-3-3 with signaling proteins is mediated by the recognition of phosphoserine. *Cell* **84,** 889–897
74. Tzivion, G., Luo, Z. J., and Avruch, J. (2000) Calyculin A-induced vimentin phosphorylation sequesters 14-3-3 and displaces other 14-3-3 partners *in vivo*. *J. Biol. Chem.* **275,** 29772–29778
75. Tzivion, G., Luo, Z., and Avruch, J. (1998) A dimeric 14-3-3 protein is an essential cofactor for Raf kinase activity. *Nature* **394,** 88–92
76. Zuzarte, M., Heusser, K., Renigunta, V., Schlichthörl, G., Rinné, S., Wischmeyer, E., Daut, J., Schwappach, B., and Preisig-Müller, R. (2009) Intracellular traffic of the K^+ channels TASK-1 and TASK-3. Role of N- and C-terminal sorting signals and interaction with 14-3-3 proteins. *J. Physiol.* **587,** 929–952
77. Rajan, S., Preisig-Müller, R., Wischmeyer, E., Nehring, R., Hanley, P. J., Renigunta, V., Musset, B., Schlichthörl, G., Derst, C., Karschin, A., and Daut, J. (2002) Interaction with 14-3-3 proteins promotes functional expression of the potassium channels TASK-1 and TASK-3. *J. Physiol.* **545,** 13–26
78. Lee, I. H., Campbell, C. R., Cook, D. I., and Dinudom, A. (2008) Regulation of epithelial Na^+ channels by aldosterone. Role of Sgk1. *Clin. Exp. Pharmacol. Physiol.* **35,** 235–241
79. Liang, X., Peters, K. W., Butterworth, M. B., and Frizzell, R. A. (2006) 14-3-3 isoforms are induced by aldosterone and participate in its regulation of epithelial sodium channels. *J. Biol. Chem.* **281,** 16323–16332
80. Ichimura, T., Yamamura, H., Sasamoto, K., Tominaga, Y., Taoka, M., Kakiuchi, K., Shinkawa, T., Takahashi, N., Shimada, S., and Isobe, T. (2005) 14-3-3 proteins modulate the expression of epithelial Na^+ channels by phosphorylation-dependent interaction with Nedd4-2 ubiquitin ligase. *J. Biol. Chem.* **280,** 13187–13194